

## Review

Anode-free sodium metal batteries  
as rising stars for lithium-ion alternativesTingzhou Yang,<sup>1,3</sup> Dan Luo,<sup>1,2,3</sup> Yizhou Liu,<sup>2</sup> Aiping Yu,<sup>1,\*</sup> and Zhongwei Chen<sup>1,\*</sup>

## SUMMARY

**With the impact of the COVID-19 lockdown, global supply chain crisis, and Russo-Ukrainian war, an energy-intensive society with sustainable, secure, affordable, and recyclable rechargeable batteries is increasingly out of reach. As demand soars, recent prototypes have shown that anode-free configurations, especially anode-free sodium metal batteries, offer realistic alternatives that are better than lithium-ion batteries in terms of energy density, cost, carbon footprint, and sustainability. This Perspective explores the current state of research on improving the performance of anode-free Na metal batteries from five key fields, as well as the impact on upstream industries compared to commercial batteries.**

## INTRODUCTION

The exponential growth of global energy consumption has driven the rapid development of renewable energy technologies to achieve sustainable development goals.<sup>1</sup> Since the discovery of electricity, a wide array of storage technologies have been developed to meet changing energy demands and technological advancements.<sup>2–4</sup> Among them, powerful lithium-ion devices are the enablers of the energy transition, especially in the field of electric vehicles (EV) and grid storage, which are expected to reach a market size of \$129.3 billion by 2027 with a compound annual growth rate of 18%.<sup>5,6</sup> As essential raw materials in lithium-ion (Li-ion) batteries, Cobalt (Co) and Li are in greater demand than other elements due to their limited distribution and low abundance.<sup>7–9</sup> Recent concerns regarding the impact of price increases on Li-ion battery production and the future of raw material supply availability have promoted the development of cheaper, more environmentally friendly alternatives, such as sodium-ion (Na-ion) batteries.<sup>10–13</sup> In 2021, the battery manufacturer CATL has launched Na-ion products online, and the existing chemistries are poised to see advances in commercial production.<sup>14</sup>

Sharing a similar working principle to Li-ion batteries, the commercial Na-ion batteries exhibit competitive low-cost advantages and exceptional electrochemical properties, which can go from 80% charge in 15 min and maintain 90% of its nameplate capacity at  $-20^{\circ}\text{C}$ .<sup>11–13</sup> However, the reported commercial Na-ion batteries still suffered from the limited energy densities of  $160\text{ Wh kg}^{-1}$ , which is only 50%–80% of that of commercial Li-ion batteries, hindering their practical applications in the large-scale energy storage market. During the 2020 T Battery Day event, Elon Musk announced to great fanfare that Model Y production will soon be powered by the new cylindrical 4680 battery.<sup>15</sup> As the name implies, the new jumbo cell will increase the energy and power due to its larger format and more materials, but the most essential energy density and safety will not be greatly improved. To achieve higher energy densities, improved battery designs are desperately sought. Fewer configurations and components mean lower cost, mass, and volume of storage systems.<sup>16</sup> Recently, anode-free configurations, which use bare current collectors at the negative electrode without any excess alkali metal, have attracted increasing attention due to their lower cost, highest volumetric energy density, and improved safety issues during battery production.<sup>17–23</sup> Compared to the conventional powerful Na-ion devices, the removal of the anode materials is feasible and will maximize the gravimetric and volumetric energy densities of batteries.<sup>24</sup> In addition, the anode manufacturing process including synthesizing, mixing, coating, and drying can be easily avoided, and the absence of the Na-ion insertion process further reduces the thickness and weight of the whole cell.

This Perspective provides an overview of the current contributions to the practical development of anode-free Na metal batteries and set out a conceptual framework for comparing with other Li-ion battery alternative chemistries. We further analyze the impact of anode-free Na metal battery commercialization on upstream industries, challenging the dominance of Li-ion batteries in mass markets. We hope this

<sup>1</sup>Waterloo Institute for Nanotechnology, Department of Chemical Engineering, University of Waterloo, 200 University Ave. W., Waterloo, ON N2L 3G1, Canada

<sup>2</sup>School of Information and Optoelectronic Science and Engineering, South China Normal University, Guangdong, 510006, China

<sup>3</sup>These authors contributed equally

\*Correspondence: [aipingyu@uwaterloo.ca](mailto:aipingyu@uwaterloo.ca) (A.Y.), [zhwchen@uwaterloo.ca](mailto:zhwchen@uwaterloo.ca) (Z.C.)  
<https://doi.org/10.1016/j.isci.2023.105982>



Anode-free configurations		Poor  Ideal				
	LIBs	LMBs	Anode-free LMBs	SIBs	SMBs	Anode-free SMBs
<b>Anode</b>	Graphite	Li metal	/	Hard Carbon	Na metal	/
<b>Anode CC</b>	Cu foil	Cu foil	Cu foil	Al/Cu foil	Al/Cu foil	Al/Cu foil
<b>Specific energy</b>	~150-260 Wh/kg	~350 Wh/kg	~380 Wh/kg	~90-160 Wh/kg	~250 Wh/kg	~300 Wh/kg
<b>Energy density</b>	~250-500 Wh/l	~750 Wh/kg	~940 Wh/l	~250-375 Wh/l	~ 530 Wh/l	~680 Wh/l
<b>Thickness</b>						
<b>Cost</b>						
<b>Safety</b>						
<b>Carbon footprint</b>						
<b>Cycle lifespan</b>						
<b>Hot spot</b>						
<b>Sustainability</b>						
<b>Market share</b>						

**Figure 1. Anode-free battery chemistries**

The comparison for Li-ion battery (LIB) alternatives, including Na-ion batteries (SIBs), Li metal batteries (LMBs), Na metal batteries (SMBs), and anode-free configurations, each with different anode current collector (CC), chemistries, and structures. The reduction in mass and volume that come with using or not using metal foils in the place of the carbon-based anode is evident, and there are some compromises and tradeoffs with different battery chemistries.

Perspective will assist the battery research and manufacturing communities in hastening the development of these anode-free configurations toward more sustainable energy storage technology.

### ADVANTAGES OF ANODE-FREE CONFIGURATION

For commercial Na-ion batteries, the fact that Na does not intercalate into graphite has led to disordered carbons becoming the preferred anode material.<sup>25</sup> Recently, metallic Na with low redox potential and high theoretical specific capacity is considered a promising anode candidate that can greatly increase the energy density of full cells by approximately 35-50% (Figure 1).<sup>26</sup> However, poor reversibility of bulk Na anodes, followed by loose stacking and severe dendrite growth, hinders the practical applications of these batteries. As such, Na metal anode plays a double game in batteries. In the last two years, the anode-free configuration, where all the active metallic ions were initially stored in the cathode material, is a milestone in minimizing cost, simplifying manufacturing processes, reducing carbon footprint, and increasing energy density.<sup>27</sup> Especially for powerful Na-ion devices, the anode-free configuration is an intriguing and under-explored possibility to boost its Na-ion cell density.

### Limitations of Na foil

Due to its highest hardness among alkali metals, metallic Li can be easily rolled and cut into different types such as plates, foils, and bars. To obtain the thin Li foil with a thickness of 50  $\mu\text{m}$  or less, more than six calendaring steps are required with the assistance of processing aids, resulting in a high cost for production.<sup>28</sup> Compared with metallic Li, metallic Na has a lower hardness, which is very difficult to handle. Even today, commercial Na foil is still not available on the market. In the laboratory, Na foil is made as follows: 1) Metallic Na blocks are dried with filter paper to remove the mineral oil and then sliced with a scalpel blade. 2) Na slices are sandwiched between two plastic films and calendared them into the thinner foil. 3) Na foil is cut into desirable sizes and used right away. It is hard to get a perfectly smooth foil, and the blades and hammers can be easily contaminated with metallic Na due to their high viscosity and reactivity, affecting the next cutting process. Due to technical limitations, the excess Na caused by the high thickness of home-made Na foil will negate the energy density advantage of Na metal anodes. Furthermore, pure sodium

metal is extremely hazardous and very sensitive even to trace moisture levels.<sup>29</sup> Some traces of moisture on our skin can react with Na to cause serious burns. Fires produced by the reaction of Na cannot be extinguished with water or carbon dioxide. Metallic Na must be stored and transported under specific conditions, away from any ambient air or moisture. Even trace amounts of moisture in mineral oil can corrode the surface of Na blocks. Before use, the metallic Na must be cleaned to remove the sodium oxide or sodium superoxide that forms a coating on the outside of metallic Na blocks.<sup>29</sup> The anode-free configurations shatter the above constraints that make the commercialization of Na metal batteries possible. The first charging process can electrodeposit Na ions onto the Al/Cu foil. During the following discharging process, the *in situ* plated Na metal dissolves again and intercalates into the cathode.<sup>16–24</sup> The concerns regarding the processing difficulties (metallic Na is pretty reactive and sticky) and low demands (since commercial Na-ion batteries are very rare) are not as overwhelming. By pairing a fully sodiated cathode material with a bare current collector (Cu or Al foil) on the anode side, both cathode and anode electrodes can remain at the same capacity after the first deposition process, yielding the maximum possible energy density compared with any other battery systems.<sup>24</sup>

### Energy density

Unlike Tesla 4680 batteries using increased volume and materials to achieve higher energy and power, anode-free configurations without any Na-ion insertion hosts at the anode side operates as a Na metal battery after the initial charging process, thus providing a higher ( $\sim 0.1$  V) operating voltage and significantly increasing both volumetric and gravimetric energy density due to the reduction in battery volume and weight.<sup>16–20</sup> Taking a Li-ion battery with the same cell parameters ( $\sim 150$  Wh  $\text{kg}^{-1}$ ) as an example, we consider cells with cathode and anode thicknesses of 85 and 110  $\mu\text{m}$ , respectively. Replacing the graphite-based anode with a 20% excess Li metal will change the thickness of the anode material to 30  $\mu\text{m}$ , resulting in 50% and 35% increases in energy density and specific energy at the cell level, respectively (Figure 1).<sup>6,22,30</sup> When Li metal or graphite-based materials are removed, the gravimetric energy density, volumetric energy density, and specific energy of anode-free configurations will increase by more than 38%, 88%, and 45%, respectively. For Na-ion batteries, the cell is assembled using a Prussian white cathode and hard carbon anode with thicknesses of approximately 90 and 120  $\mu\text{m}$ .<sup>25,31</sup> The anode thickness will be reduced by 20  $\mu\text{m}$  when paired with 20% excess Na metal, and the removal of anode materials, which occupy 44.7% of the overall thickness, would boost the volumetric energy density by 81%.<sup>32</sup> Significantly, anode-free configurations still suffer from large volume changes during the reversible electrochemical process, especially for Na-ion-based strategies. Even excluding the negative effect of volume changes, the energy density is still greatly improved compared with traditional batteries. Furthermore, the energy density also depends on the cell and electrode design. The increased thickness of the cathode will result in an increased energy density and reduced rate performance. This capacity-rate tradeoff can be improved by electrical conductivity, electrode thickness, porosity, and tortuosity. As with 4680 cells, the high-energy cells are designed with a thick electrode coating, while high-power cells require thin electrodes to prevent transport limitations during the fast-charging process. Both conventional Na-ion batteries and Na metal batteries are moving toward their limits, and anode-free configurations will further overcome the limit of this extreme value.

### Carbon footprint and costs

Unlike rarer Li (0.0065% of the Earth's crust), Na is the principal cation in seawater and extracellular fluids, accounting for around 2.36% of the Earth's crust in compound form.<sup>33</sup> Li is a by-product of the mining of other elements, and the brine deposits that produce Li today are mainly found in Chile, with reported concentrations of Na and Li of about 9.1 wt % and 0.157 wt % respectively. Similar to Li, the production of cobalt (Co) is a strong dependency on the mining of copper (Cu) and nickel (Ni), which are located in the politically unstable border region between Congo and Zambia.<sup>34</sup> Significantly, China and Japan occupy more than 95% of anode materials sales worldwide, and the battery manufacturers are mostly headquartered in Asian countries.<sup>35,36</sup> This supply chain is long and complicated with carbon emissions, environmental waste, energy consumption, shipping, and logistics, further increasing the carbon footprint and cost. Na cannot be found freely in nature due to their high reactivity, and the low-cost and highly abundant Na salts including  $\text{Na}_2\text{CO}_3$ , NaCl, and  $\text{Na}_2\text{SO}_4$  can be obtained directly from minerals and brine, resulting in a low carbon footprint.<sup>34</sup> Metallic Na is produced by the electrolysis of a molten mixture of sodium chloride and calcium chloride. The cathode materials for Na-ion batteries are mainly focused on transition metal layered oxides, polyanionic compounds, and Prussian blue analogs, which are essentially composed of elements that are relatively abundant in the earth, such as Fe, Mn, V, P, N, and O. We further compared the cost percentages

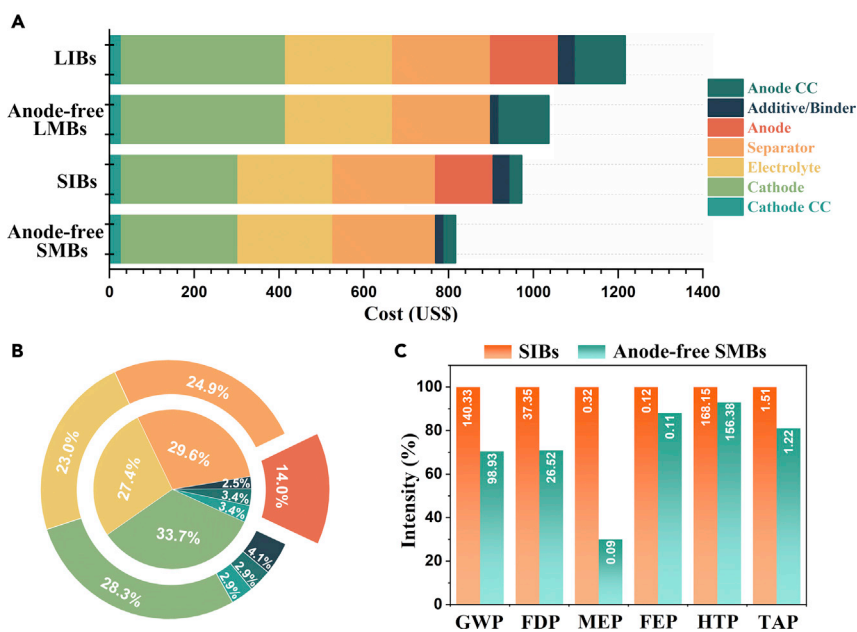


**Figure 2. Cost comparison and environmental impact of different configurations**

(A) Cost breakdown of different compositions for six modeled different battery configurations.

(B) Cost ratios of different compositions for Na-ion battery (external) and anode-free Na metal battery (internal).

(C) The global warming potential (GWP), fossil depletion potential (FDP), marine eutrophication potential (MEP), freshwater eutrophication potential (FEP), human toxicity potential (HTP), terrestrial acidification potential (TAP) for the production of 1kWh of Na-ion battery and anode-free Na metal battery.

of different components between Li-ion batteries, Na-ion batteries, and anode-free configurations by a 7 kW, 11.5 kWh battery system.<sup>32</sup> The estimated models show that the anticipated cost of a Na-ion battery based on advanced hard carbon (\$973.0) is much lower than for a Li-ion battery based on synthetic graphite (\$1217.0). For anode-free configurations, the costs are further reduced to \$1037.0 and \$817.0, which are about 14.8% and 32.9% cheaper compared to Li-ion batteries, respectively (Figures 2A and 2B). More importantly, the anode-free Na metal batteries can save the cost associated with Cu-based current collector and hard carbon production, further avoiding the use of organic solvents and simplifying the production steps of mixing, coating, and drying. In Na-based batteries, the use of cyclic carbonates or ether-based solvents and additives such as fluoroethylene carbonate increases the cost of the electrolytes, but Na salts are much cheaper than Li salts.<sup>37</sup> Moreover, the energy consumption and greenhouse gas emissions during the battery value chain are reduced by 11.5% and 7.4%. The global warming potential (GWP) and fossil depletion potential (FDP) of Na-ion batteries was about 140.33 kg CO<sub>2</sub>-eq and 37.35 kg oil-eq for the production of 1 kWh of storage capacity, where the anode-free configuration will reduce the total FDP and GWP by about 29% (Figure 2C). In addition, nearly 11.77 kg 1,4-DCV-eq and 0.29 kg SO<sub>2</sub>-eq emissions will be eliminated, accounting for 7% and 19% of the total human toxicity potential (HTP) and terrestrial acidification potential (TAP).<sup>31</sup> Furthermore, the anode-free configuration is well compatible with the current applied Li-ion battery manufacturing infrastructure, avoiding the waste of haphazard investment and redundant construction.

### Sustainability

Sustainable development goals encourage us to develop closed-loop energy storage systems with a circular economy. For the recycling of conventional batteries, the outer shells, current collectors, separator, cathode materials, and anode materials can be easily separated through crushing and screening after dismantling due to their different physical properties. A mixture of cathode and anode material powders can be obtained, called black mass.<sup>9</sup> For alkali metal batteries, special precautions are required during the disassembly and further processing, such as shredding, crushing, and sieving, due to the high reactivity and viscosity of metallic Li/Na, which may lead to rapid exothermic reactions.<sup>35,36</sup> The scrap Al and Cu can be recycled by a simply re-melting step, either to the finished shape or for subsequent fabrication. For pure

cathode materials, a direct cathode recycling method is proposed, which can minimize the costs, reduce carbon footprints, and alleviate raw material shortages, in case the cathode materials would not have been resynthesized from the raw materials or precursors. Furthermore, chemical methods based on pyrometallurgy, hydrometallurgy, and biometallurgy are used to extract the metal contained in the cathode, and research based on extraction, precipitation, coordination chemistry, and ion exchange are used to separate each metal element.<sup>35,36</sup> Nowadays, most of the anode materials are destroyed by burning or collected as precipitates after filtration during recycling. Due to the existence of Li/Na residue and the structural collapse of the carbon materials, the regeneration of the recovered carbon material as the new anode material is not feasible. For anode-free configurations, no anode active materials are required and the thin Li/Na layer deposited on the surface of the current collector can be removed during the discharged state. Such recycling would be simplified dramatically in the case of anode-free configurations. Both cathode and anode-side current collectors are Al foil, which greatly simplifies the separation process. With the support of direct cathode recycling, this would significantly reduce carbon footprint, energy consumption, and process cost, which allows closed-loop recycling of anode-free Na metal batteries.

### IMPACT ON UPSTREAM INDUSTRIES

The commercialization of Na-ion batteries and the development of anode-free Na metal batteries will have varying degrees of impact on different battery components, especially for the cathode and current collector. The growing demand for cathode materials in Na-ion batteries has created immense opportunities for upstream industries such as transition metals and sodium carbonate ( $\text{Na}_2\text{CO}_3$ ), thus augmenting the market value. The use of an Al current collector for both cathode and anode sides is expected to boost the demand for Al foils. The impact on other components is minimal. The production of Al plastic film and electrode tabs is the same as that used in Li-ion batteries. Existing commercial separators based on glass fiber or PP/PE composites meet the requirements of anode-free Na metal batteries with large pore sizes to ensure the migration of solvation structures during cycling.

### Transition metal

For anode-free Li metal batteries, the demand for transition metals is mainly concentrated in Co, Ni, and Mn. The global transition metal market is anticipated to exhibit a CAGR of over 4.2% and reach around \$1,369.46 billion by the end of 2028. Co is a relatively rare element of the earth's crust, mainly found in Ni-bearing laterite deposits and Ni-Cu sulfide deposits (Figure 3A). The Democratic Republic of Congo is the world's largest producer of Co accounting for 70% of global production, followed by Russia and Australia.<sup>34</sup> With the explosive growth in global demand for Li-ion batteries, so has the price of Co (Figure 3B). Some uncertainty can be generated by environmental pollution, political instability, corruption, looting, and mineral smuggling, in particular child labor and lack of safety measures. Russia's invasion of Ukraine in 2022 is expected to affect global Co supply and prices with an adverse reaction to the operation of the global supply chain. More than two-thirds of global Ni production is used to produce stainless steel, and others are used in manufacturing Li-ion batteries. Since 2018, the US-China trade war and COVID-19 pandemic softened the impact of the Brumadinho dam catastrophe in Brazil and the high demand from the stainless-steel sector in China. Economic recovery after the COVID-19 pandemic will increase the global nickel demand to 3.05 million mt in 2022. Russia's invasion of Ukraine in 2022 could weigh on global Ni supply and the global supply in the near term could tighten due to the increased power costs caused by higher natural gas prices, where the nickel contract trading price on the London Metal Exchange hit a historic high on March 8.<sup>38,39</sup> The application of anode-free Na metal batteries will significantly reduce the demand for Ni and Co. For commercial Na-ion batteries, CATL used Prussian white material as the cathode materials, and some spin-offs including HiNa Battery, Tiamat, and Faradion have performed tests on the pouch or cylindrical cells with  $\text{Na}_{0.9}\text{Cu}_{0.22}\text{Fe}_{0.3}\text{Mn}_{0.48}\text{O}_2$ ,  $\text{Na}_3\text{V}_2(\text{PO}_4)_2\text{F}_3$ , and  $\text{Na}_x\text{Ni}_{1-x-y-z}\text{Mg}_x\text{Mn}_y\text{Ti}_z\text{O}_2$  cathode materials (composed of earth-abundant elements such as Fe, Mn, and V), which are mainly focused on transition metal layered oxides, polyanionic compounds, and Prussian blue analogs. The most studied families of cathode materials for anode-free Na metal batteries are presodiated  $\text{FeS}_2$ ,  $\text{Na}_3\text{V}_2(\text{PO}_4)_3$ , and  $\text{Na}_2\text{Fe}_2(\text{CN})_6$ . According to the HiNa Battery's report, the cost of  $\text{Na}_{0.9}\text{Cu}_{0.22}\text{Fe}_{0.3}\text{Mn}_{0.48}\text{O}_2$  cathode is only 40% of  $\text{LiFePO}_4$  cathode. In terms of crustal abundance, Fe is the most abundant transition metal, ranking fourth among all elements and second among metals after Al. As the 12<sup>th</sup> most abundant element, Mn reserves are about 570 million tonnes and distributed in different countries.<sup>34</sup> V is the 20<sup>th</sup> most abundant element in the earth's crust, and its compounds occur naturally in about 65 different minerals and fossil fuels (Figure 3A). More than 97% of produced V is mined from South Africa, China, and Russia.<sup>34</sup> The global abundant Fe, Mn, and V reserves can meet the growing demand for anode-free Na metal batteries in the future,

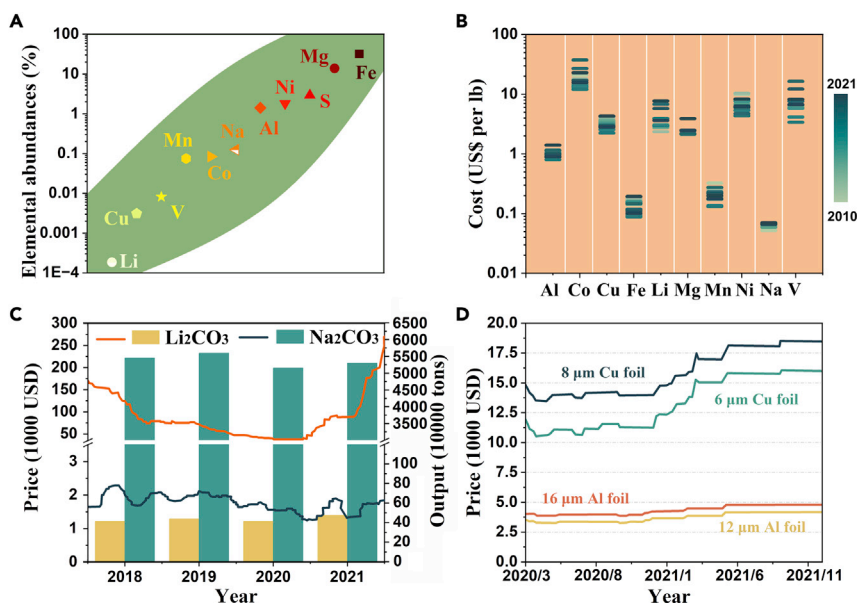


**Figure 3. Impacts on upstream industries**

Different battery configurations affect the corresponding upstream industries, depending on the availability of key materials and geological resources.

(A) Abundance of elements used in battery chemistry on Earth.

(B) Average prices of corresponding critical metals from 2010 to 2021.

(C) Annual global production and cost of Lithium Carbonate (Li<sub>2</sub>CO<sub>3</sub>) and Sodium Carbonate (Na<sub>2</sub>CO<sub>3</sub>), indicating the advantages of Na-ion batteries and anode-free Na metal batteries.

(D) As the most common choice, Cu foil, and Al foil are used as positive and negative current collectors, whereas anode-free Na metal batteries use Al foil on both sides. The price of battery-grade Al foil is much lower than that of copper foil.

even replacing low energy density Li-ion batteries, without causing the same price spikes as Li and Co. The commercialization of anode-free Na metal batteries will have a great impact on existing upstream industries of Li-based cathode materials such as non-ferrous metals and chemical products. However, the ultimate impact is uncertain as which cathode materials will be the “holy grail” remains unknown. At present, the industrialization rate of Na-ion batteries is low, and corresponding cathode technology routes are clearly differentiated, which cannot fully reflect the cost advantages of Na-ion batteries. With continuous modification and scale production, the cost of cathode materials for anode-free Na metal batteries will be greatly reduced.

### Sodium carbonate

There must be a source of Na in different systems for anode-free configurations. According to the reported production method, sodium hydroxide, sodium carbonate (Na<sub>2</sub>CO<sub>3</sub>), sodium bicarbonate, sodium acetate, sodium oxalate, sodium citrate, and sodium nitrate are used to synthesize cathode materials for anode-free Na metal batteries while NaClO<sub>4</sub>, NaPF<sub>6</sub>, NaTFSI, and NaCF<sub>3</sub>SO<sub>3</sub> have been proposed as the Na salts in the electrolytes.<sup>40</sup> Among them, sodium hydroxide and Na<sub>2</sub>CO<sub>3</sub> are the most common sources of Na, and Na<sub>2</sub>CO<sub>3</sub> can also be used as the starting material to synthesize these Na salts. Na<sub>2</sub>CO<sub>3</sub>, also known as soda ash, is prepared with the help of the Solvay process or derived from a series of refining steps of trona ore. As one of the most common and important industrial chemicals in North America, it is used in laundry detergent, paper manufacturing, and glass manufacturing. Rising infrastructure investments and significant economic growth have led to a booming construction industry, thereby driving the demand for Na<sub>2</sub>CO<sub>3</sub> as an important raw material. Glass production accounts for more than 50% of global Na<sub>2</sub>CO<sub>3</sub> demand. With growing environmental consciousness and expansion of the food and beverage sector, replacing plastic containers with glass containers will further stimulate the growth of the Na<sub>2</sub>CO<sub>3</sub> market (Figure 3C). Over half of soda ash is produced in Asia, and the USA is the world’s largest producer of natural soda ash, of which only 42.3% is consumed by domestic companies.<sup>34</sup> In addition, for Li-ion batteries, the global lithium carbonate (Li<sub>2</sub>CO<sub>3</sub>) output is estimated to total 410,000 metric tons in 2021, and the average

price of battery-grade  $\text{Li}_2\text{CO}_3$  was estimated at \$17,000 per metric ton (Figure 3C). Driven by the drastic growth of the energy storage market, the  $\text{Li}_2\text{CO}_3$  market will re-enter a period of undersupply in 2025, where the global demand is expected to surpass 861,000 metric tons with a CAGR of 20%. According to SNE Research, the total battery market for EVs was around 296.8 GWh,<sup>41</sup> more than double the previous year. As promising alternatives to commercial Li-ion batteries, anode-free Na metal batteries with an energy density of 250-400 Wh  $\text{kg}^{-1}$  have the potential to replace the most powerful batteries on the current market, which means that the potential market for anode-free Na metal batteries is around 296.8 GWh in 2021. According to different existing cathode materials for Na-ion batteries, the corresponding demand for battery-grade  $\text{Na}_2\text{CO}_3$  is about 170,000-870,000 metric tons. In 2021, the total global production for  $\text{Na}_2\text{CO}_3$  was estimated at 59 million metric tons, accounting for only 80% of the existing capacity.<sup>34</sup> The global synthetic  $\text{Na}_2\text{CO}_3$  market is slated to be just over \$13.5 billion, registering a CAGR of 3% from 2021 to 2027. The existing production capacity can fully meet the new demand for the energy storage market, and the price of  $\text{Na}_2\text{CO}_3$  is only 0.34% of the price of  $\text{Li}_2\text{CO}_3$ .

### Aluminum foil

Anode-free Na metal batteries allow the use of Al foil as a current collector on both anode and cathode sides which doesn't form a binary alloy with Na, further reducing the cost of anode-free configurations.<sup>19,24</sup> In 2020, the global Al foil market size was valued at \$24.09 billion with an expected CAGR of 6.0% from 2021 to 2028. Whether for technical applications or packaging such as the insulation of power cables or the containers of food-Al foil offers countless possibilities and is indispensable in any branch of the industry. In 2021, China's Al foil production was expected to reach 4.33 million tons, and the output of battery-grade Al foil reached 70,000 tons.<sup>34,42</sup> With the rapid development of the EV market, the boom in the Al foil and Cu foil industry has followed (Figure 3D). For battery-grade Cu foil, the price of Cu as of March 2022 is around \$10,000 per ton, and processing Cu foils to 8.0  $\mu\text{m}$ , 6.0  $\mu\text{m}$ , and 4.5  $\mu\text{m}$  required additional cost, about \$4,800, \$7,200, and \$11,200, respectively. The price of Al ingot is only \$3,600 per ton, and the manufacturing overhead for battery-grade 16.0  $\mu\text{m}$  and 12.0  $\mu\text{m}$  Al foils is about \$900 and \$1,500.<sup>42</sup> So the cost of the current collector in a Na-ion battery is only 4% of the total cost, compared to 15% in a Li-ion battery (Figure 3D). Sharing similar performance requirements to Li-ion batteries with a high technical threshold, battery-grade Al foil manufacturers will benefit from the future development of anode-free Na metal batteries and continue to maintain their first-mover advantage. Recently, the strength of Al foil is greater than 180 MPa, which is comparable to the performance of 8-series alloys. The thickness of Al foil is required to be thinner, reaching 8.0  $\mu\text{m}$ , which has exceeded the current minimum limit thickness of single-piece rolling of Al foil products. In China, some manufacturers have unveiled that commercial battery-grade 4.0  $\mu\text{m}$  Al foil is available. Furthermore, surface modification technology of Al foil has been designed to reduce the interface resistance, protect the current collectors, reduce the polarization and improve the battery performance. The carbon coating process with a surface loading of 0.5-2.0  $\text{g m}^{-2}$  has been successfully commercialized. At present, the consumption of battery-grade Al foil is around 600-800 tons  $\text{GWh}^{-1}$ . As the alternative to the  $\text{LiFePO}_4$ -based batteries, the potential market capacity for anode-free Na metal batteries is expected to be around 450 GWh, corresponding to a battery-grade Al foil demand of 720,000 tons. Driven by their use in a wide range of energy storage systems, the actual demand for aluminum foils will be greater.

## MAIN CHALLENGES AND STRATEGIES FOR OPTIMIZATION

Although anode-free Na metal batteries show much promise due to their enhanced energy density and design simplicity, achieving long cycle life remains a formidable challenge, where only 80% of capacity can be reserved within 20 cycles. The performance degradation can be attributed to the limited Na source and irreversible Na loss through severe parasitic reactions.

### Limited Na source

For conventional batteries, the Na metal anode has excess Na ions and we can use sodiated hard carbon-based materials to replenish Na-ion loss on the anode side before assembly. For the anode-free configurations, Na ions in the cathode materials and electrolytes are the only available Na source, and only about 20% of the extracted Na is recovered back into the cathode materials during the initial discharge processes in an unmodified system. How to increase the number of Na ions in the system is particularly important for anode-free Na metal batteries.

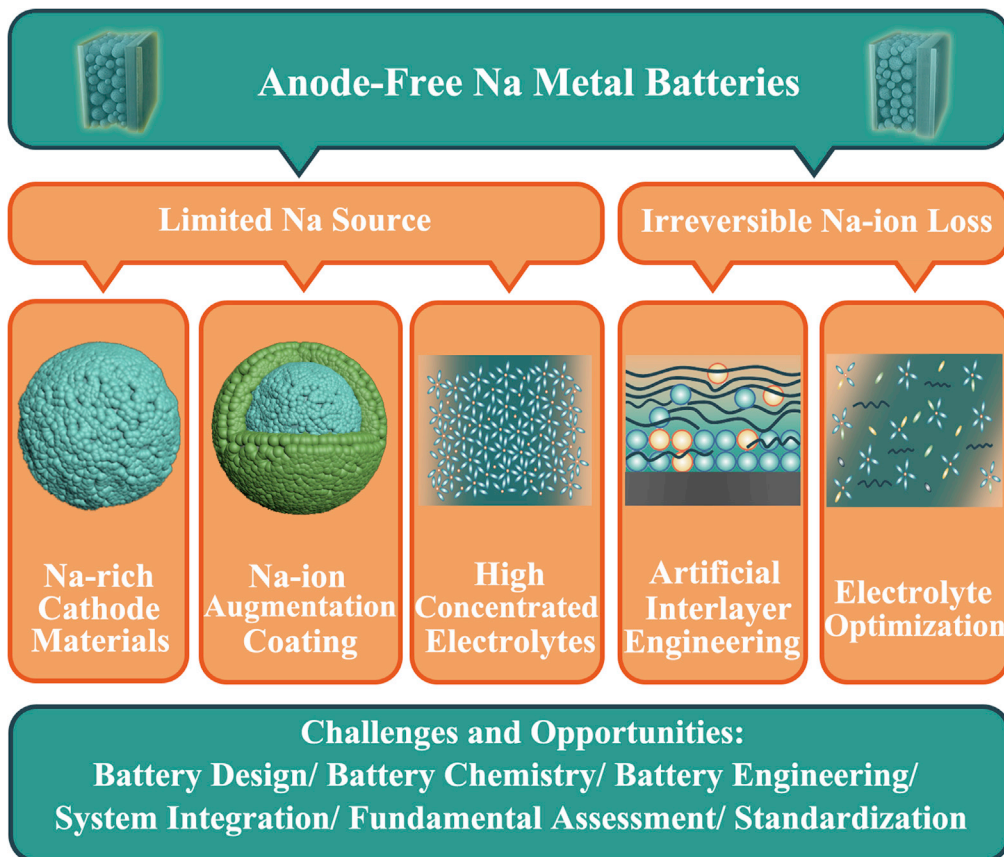


**Figure 4. Major development progress of anode-free configurations**

The optimization strategies for anode-free Na metal batteries mainly focus on the Na-rich cathode materials, Na-ion augmentation coating, artificial interlayer engineering, and optimization of electrolyte formulations. To meet the benchmark requirements for commercialization, some challenges still need to be addressed.

#### *Na-rich cathode material*

Na-rich cathode materials are the first choice for compensating the Na loss and improving the energy density of anode-free configurations (Figure 4). In the field of anode-free Li-based configurations, Lin et al. found that the Li-rich  $\text{Li}_2\text{Ni}_{0.8}\text{Co}_{0.1}\text{Mn}_{0.1}\text{O}_2$  cathode can serve as the Li-ion extender to prolong the lifespan of anode-free Li metal batteries.<sup>43</sup> During the first charging process, the excess Li ions from the Li layer are deposited on the surface of Cu foil and  $\text{Li}_2\text{Ni}_{0.8}\text{Co}_{0.1}\text{Mn}_{0.1}\text{O}_2$  cathode can be reversibly converted into conventional  $\text{LiNi}_{0.8}\text{Co}_{0.1}\text{Mn}_{0.1}\text{O}_2$  cathode. After that, it will function as a conventional  $\text{LiNi}_{0.8}\text{Co}_{0.1}\text{Mn}_{0.1}\text{O}_2$  cathode and work steadily in future cycles.<sup>44,45</sup> A similar strategy based on Li-rich  $\text{Li}_2\text{Ni}_{0.5}\text{Mn}_{1.5}\text{O}_4$  cathode was reported by the same group, which makes this concept attractive for developing anode-free Na metal batteries. Na-rich cathode materials are considered the next-generation cathodes due to their high rechargeable capacity and average discharge potential that can replenish Na ions in anode-free configurations. So far, 4d/5d metal-based O3-type layered materials have been found for Na-rich materials with anionic redox activity, and the representative systems include Na-rich layered  $\text{Na}_x\text{TMO}_y$  ( $x, y \geq 2$ ) cathodes including  $\text{Na}_2\text{RuO}_3$ ,  $\text{Na}_2\text{SeO}_3$ ,  $\text{Na}_2\text{ZrO}_3$ ,  $\text{Na}_2\text{Ru}_{1-x}\text{Zr}_x\text{O}_3$ ,  $\text{Na}_2\text{Ru}_{1-x}\text{Mn}_x\text{O}_3$ , and  $\text{Na}_{1.2}\text{Mn}_{0.4}\text{Ir}_{0.4}\text{O}_2$ .<sup>46–49</sup> It is worth noting that the lack of continuous covalent bonding between transition metals and metastable peroxo-like species may induce a series of consequences, such as side reactions with electrolytes,  $\text{O}_2$  release, and transition metal migration. Some possible solutions, such as mixing 3days metal with 4d/5d metal and increasing the M'/M ratio ( $\text{Na}_x[\text{M}'_y\text{M}_{1-y}]\text{O}_2$ ), have been reported to improve the reversibility of anionic redox materials. Various Na-rich Prussian blue analogs such as  $\text{Na}_{1.94}\text{Ni}_{1.03}\text{Fe}(\text{CN})_6$ ,  $\text{Na}_{1.4}\text{Cu}_{1.3}\text{Fe}(\text{CN})_6$ , and  $\text{Na}_{0.61}\text{Fe}[\text{Fe}(\text{CN})_6]_{0.94}$  have been reported as the cathode materials for Na-ion batteries.<sup>50</sup> Wang et al. used a controllable precipitation method at room temperature to fabricate a series of Na-rich  $\text{Na}_{2-x}\text{FeFe}(\text{CN})_6$  with a rhombohedral structure, which exhibits excellent cycling stability over 1000 times.<sup>51</sup>

Na-rich materials serve as the cathode materials and Na-reservoir simultaneously to eliminate irreversible capacity loss in anode-free configurations since they can be converted into routine cathodes and Na metal after initial formation cycles. Due to the differences in ionic radius and polarization, it is inappropriate to directly transfer the anionic redox theory from Li-rich to Na-rich cathode materials. Many challenges remain, such as O<sub>2</sub> release, transition metal migration, voltage fade, and side reactions with electrolytes, which should be addressed to facilitate the development of Na-rich cathode materials for anode-free configuration.

### Na-ion augmentation coating

Recently, some works show that the Li-doping approach is used to compensate for the initial irreversible capacity loss of cathode materials, where the additional Li additives including Li<sub>2</sub>MoO<sub>3</sub>, Li<sub>2</sub>RuO<sub>3</sub>, Li<sub>6</sub>CoO<sub>4</sub>, Li<sub>2</sub>CuO<sub>2</sub>, Li<sub>5</sub>ReO<sub>6</sub>, LiFeO<sub>2</sub>, Li<sub>2</sub>O, Li<sub>2</sub>S, Li<sub>2</sub>CO<sub>3</sub>, Li<sub>3</sub>N, Li<sub>3</sub>P, LiCl, and LiF are incorporated into conventional cathode materials as the extra Li-ion source.<sup>52</sup> For instance, Zhang et al. used Li-rich Li<sub>2</sub>CuO<sub>2</sub> to obtain a thin Li metal layer onto the Cu current collector, which serves as the primer layer for the next Li cycling in the battery, further enhancing the rate capability of LiNi<sub>0.8</sub>Mn<sub>0.1</sub>Co<sub>0.1</sub>O<sub>2</sub> cathode and exhibiting capacity retention of more than 85% for 120 cycles.<sup>53</sup> A similar strategy was reported by Park et al. that a solid solution of Li<sub>2</sub>MoO<sub>3</sub> with LiFeO<sub>2</sub> cathode exhibits a stable crystalline structure at the charged states, further suppressing the dissolution of Mo ions and improving the electrochemical performance in the operating voltage range of 0.0–4.3V.<sup>54</sup> Sharing a working principle similar to Li-based batteries, Ye et al. showed that an artificial Na-rich cathode-electrolyte interface is designed on a Prussian blue cathode,<sup>55</sup> which consists of organic Na-based species (R-Co-Na, R-O-Na, and R-O<sub>2</sub>CO-Na) and inorganic Na-salts (NaF, NaCl, Na<sub>2</sub>CO<sub>3</sub>, and NaHCO<sub>3</sub>). As an excellent ionic conductor and electronic insulator, the Na-ion augmentation coating can allow the fast transport of Na ions, reduce the consumption of electrolytes, and compensate for Na-ion loss in the anode-free Na metal batteries. With the gradual increase in the content of electrochemically inert Ni species from the interior to the particle surface, concentration-gradient Na<sub>x</sub>Ni<sub>y</sub>Mn<sub>1-y</sub>Fe(CN)<sub>6</sub> can deliver a high reversible specific capacity and outstanding cycling stability compared to homogeneous Na<sub>x</sub>MnFe(CN)<sub>6</sub> due to the effective suppression of Jahn-Teller effect.<sup>56</sup> Gebert et al. proposed core-shell structured Na<sub>2</sub>NiFe(CN)<sub>6</sub>@Na<sub>2</sub>MnFe(CN)<sub>6</sub> cathode that nickel-rich outer layer plays an active role in stabilizing the normally electrochemically unstable Mn-rich core, further preventing the Jahn-Teller distortions it normally undergoes during desodiation.<sup>57</sup> In my opinion, Na-ion augmentation coating methods make commercial cathode materials for anode-free Na metal batteries more accessible and large-scale applications (Figure 4). Although significant improvement in electrochemical performance demonstrates the positive role of suitable Na-ion augmentation coating, there are still many factors that need to be fine-tuned for optimal results including species, thickness, defects, and uniformity of Na-ion augmentation coating on electrochemical performance for anode-free Na metal batteries.

### Superconcentrated electrolytes

Except on the cathode side, the excess Na ions can only be stored in the electrolyte, where superconcentrated electrolytes have also shown promising functionalities to provide additional Na ions and remove many of the fundamental drawbacks.<sup>58,59</sup> Furthermore, the superconcentrated electrolytes promote the increasing amount of contact ion pair and aggregates species, resulting in the growth of a favorable SEI layer and improving the electrochemical performance of anode-free Na metal batteries.<sup>60,61</sup> Notably, Qian et al. compared the performance between highly concentrated 4.0 M LiFSI-DME electrolytes and commercial 1.0 M LiPF<sub>6</sub>-EC/DMC in the Cu||LiFePO<sub>4</sub> anode-free battery, where consumed in commercial electrolyte after the first cycle and Li-ions are still reserved in high-concentrated electrolytes.<sup>62</sup> The Li-ions with a 4-fold increase in the concentration can undergo a reduction reaction on the surface of Cu foil to form metallic Li during the charging processes. Furthermore, salt anions in high-concentrated electrolytes promote the formation of a favorable SEI layer for uniform Li deposition due to the formation of a more uniform Li-ion flux. Beyene et al. reported a fluorinated concentrated electrolyte (3.0 M LiFSI-DME/DOL) for a high-voltage anode-free configuration, which can minimize parasitic side reaction and result in the formation of ROCO<sub>2</sub>Li as well as LiF-rich-flexible SEI layer.<sup>63</sup> Recently, some superconcentrated dual-salt electrolyte systems based on LiFSI and LiTFSI salts had been confirmed as an effective approach to improving anode-free battery performance.<sup>64</sup> For Na-based configuration, Hwang et al. investigated the maximum solubility of binary and ternary Na salt systems in superconcentrated electrolytes using fundamental concepts of molten salt chemistry,<sup>61</sup> which implies that the eutectic composition of ternary Na salt system achieves concentrations as high as 5.0 M into organic solvents. Sun et al. used the ionic liquid to prepare superconcentrated Na-ion electrolytes,<sup>65</sup> where the anion decomposition species in the ionic

liquid electrolyte contribute to an inorganic SEI with high ionic conductivity, further facilitating the Na desolvation and diffusion kinetics. Lu et al. designed a 3A zeolite molecular sieve film to construct a highly aggregated solvation structure through the size effect, which can extend the oxidative stability and suppress oxidative decomposition without sacrificing the Na reversibility.<sup>66</sup> For commercial applications, the cost of an anode-free configuration should be considered in advance, and some expensive salts and ionic liquids should be avoided. It is worth noting that the superconcentrated electrolytes are always corresponding to high viscosity, which will decrease the ionic conductivity and become difficult to wet separator. Recently, some works show that the diluents, such as FEC and DME, are added to the superconcentrated electrolyte systems to increase the conductivity and ionic mobility of this high-viscosity concentrated electrolyte.<sup>67</sup> The design of the new salt-solvent electrolytes for anode-free Na metal batteries should optimize the balance between the degree of Na salt dissociation, the viscosity of the electrolytes, and the strength of solvation factors, which is associated with the formation of the SEI layer and ionic conductivity of electrolytes. Furthermore, different electrolytes have different solvation structures, and the solvation effect is crucial to reducing irreversible loss of Na-ions in an anode-free configuration.

### Irreversible Na-ion loss

The limited Na sources can be depleted by the formation of the SEI layer and the growth of Na dendrite and dead Na. Specifically, Al foils serve as the only configuration on the anode side for anode-free Na metal batteries, which exhibit greatly increased nucleation overpotentials (32-81 mV) for Na deposition compared to carbon-based materials (9-37 mV). The high nucleation overpotentials are all used to overcome the heterogeneous nucleation barriers and the large overpotentials are likely to result in uneven Na deposition morphology, where Na particles are inclined to grow into the isolated Na dendrite structures, further reducing the availability of Na source and degrading the electrochemical performance. Moreover, the Na ions can easily react with electrolytes, and the decomposition of electrolytes leads to the formation of solid electrolyte interphase (SEI) layer at the surface of the anode, accompanied by an irreversible loss of Li-ions. The growth of Na dendrites accompanied by large volume changes can disintegrate the weak SEI layer and lead to repeated formation of the SEI layer, continued consumption of Li-ions, and decomposition of electrolytes. The large amounts of defects in SEI can induce uneven electric field and ions-flux, further accelerating the uncontrollable growth of Na dendrites. Artificial interlayer engineering and electrolyte modification have been employed to reduce the irreversible Na-ion loss (Figure 4).

### Artificial interlayer engineering

Alloys between Na and Al cannot be formed in the voltage range between 0.0 and 5.0 V, which allows the utilization of the Al substrate as the current collector. For anode-free Na metal batteries, replacing the Cu anode current collector with a cheaper and lighter Al current collector is more responsive to the minimalist productive process and low-cost requirements for large-scale commercialization.<sup>68,69</sup> State-of-the-art current collector designs for improving the cyclability of anode-free configurations have mainly focused on the artificial interface, where designs based on alternative, porous, or three-dimensional current collectors are not discussed later in discussion due to their inapplicability for commercial applications.<sup>70,71</sup> Surface modification with an artificial interface can block the direct contact between liquid electrolytes and deposited Na metal, further preventing the excessive Na ion loss caused by dendrite formation and heterogeneous deposition and reducing the consumption of electrode materials and electrolytes. Artificial interface or protective layers can be fabricated by physical/chemical vapor deposition, spin coating technology, self-assembly, and the formation of coordinate bonds on Al substrates. Tian et al. and Snyder et al. used first-principles calculations to investigate the practicability of different materials as artificial protection coatings, where the defect features, bond length, crystalline structures, and metal proximity effect play a crucial role in improving the protective effect in the terms of the diffusion properties and mechanical performance.<sup>72,73</sup> The materials, such as defective h-BN, graphene phosphorene, SnSe, and SnS, are not suitable for anode-free Na metal anodes, resulting in low diffusion efficiency and poor strain properties. Wang et al. constructed the  $\text{Na}_2(\text{Sb}_{2/6}\text{Te}_{3/6}\text{Vac}_{1/6})$  substrate to assemble anode-free metal batteries, which exhibit enhanced wettability of Na metal.<sup>74</sup> More than 118 promising coatings including binary, ternary, and quaternary compounds are identified that exhibit stable equilibrium with the Na metal anode.<sup>75,76</sup> Several approaches using carbon material layers, Poly(vinylidene difluoride), and pyroprotein seed layers to modify substrate surface have recently been devoted to reducing the initial nucleation barrier and guiding uniform deposition. Li et al. introduced a graphitic carbon-coated Al current collector to realize reversible and crack-free Na deposition.<sup>24</sup> Cohn et al. and Mazzali et al. assembled a nano-carbon nucleation layer on Al substrate as the current collector for anode-free Na metal batteries,<sup>77,78</sup> which serve as nucleophilic active sites to enable efficient and stable Na plating,

resulting in a high energy density of  $\sim 400 \text{ Wh kg}^{-1}$ . Tang et al. introduced a sodiophilic layer of Au-Na alloy on the substrate, where the Au sites can change the interphase chemistries of the Na metal anode, acting as lower nucleation barrier sites for Na deposition.<sup>79</sup> Recently, the application of  $\text{Al}_2\text{O}_3$  coatings as protective SEI layers via atomic layer deposition has been demonstrated to suppress the dendrites and mossy Na formation and improve the lifetime of cells.<sup>80,81</sup> Similarly, molecular layer deposition is employed to fabricate organic and inorganic-organic thin coatings via C-O and C-C bonds from the organic linkers, which can reduce dendrite growth and improve the stability in the  $\text{NaPF}_6$  contained electrolyte. Furthermore, the researchers used physical vapor deposition to construct Au, Ag, Cu, Ni, and Al patterned current collectors with different metal-pattern diameters and the distance for anode-free configurations, and the optimal ratio could facilitate the formation of thin-film Na metal layers. Li et al. constructed a robust nucleation buffer layer based on metal-organic frameworks-derived Cu-carbon composite on conventional current collectors, serving as the abundant nucleation sites to guide Na deposition and buffer volume changes.<sup>82</sup> Our previous work used metal-organic frameworks as the source to construct single atoms on the surface of substrate, which can guide the Na metal deposition, further realizing the successful cycling of "Na-less" metal batteries with N/P ratio of 100%.<sup>26</sup>

### Electrolyte modification

As a critical component of anode-free configurations, electrolyte developments follow that of conventional electrolytes with common solvents and salts, which are highly desirable for determining the morphology of the deposited Na and participating in the buildup of SEI and CEI layers.<sup>83</sup> Due to the high cohesive energy of Na salts with preferable thermal stability and safety, the electrolytes can be classified as organic and solid-state electrolytes. By precisely tuning the electrolytes, a favorable SEI layer with high ionic conductivity is formed on the deposited Na surface, suppressing undesirable side reactions. The growth of Na dendrites and dead Na can also be alleviated, thereby reducing the consumption of Na-ions during cycling. Eldesoky et al. screened 4 electrolytes out of 65 electrolyte formulations that showed a slight improvement over the baseline, where the trend in energy retention did not always correspond to the concentration of additive or co-solvent used.<sup>84</sup> Due to the high reactivity between Na metal and carbonate-based solvents, the reported anode-free Na metal batteries with liquid electrolytes mainly use diglyme as the electrolyte solvents and  $\text{NaPF}_6$ ,  $\text{NaTFSI}$ , or  $\text{NaCF}_3\text{SO}_3$  as Na salts, where the electrolytes using glymes (mono-, di-, and tetraglyme) as the solvents enable highly reversible and nondendritic stripping/plating process at room temperature. Weber et al. showed that anode-free pouch cells using 1.2 M dual-salt  $\text{LiDFOB/LiBF}_4$  liquid electrolyte deliver 80% capacity remaining for 90 cycles and a smooth dendrite-free Li morphology can be observed after multiple cycles.<sup>85</sup> Similarly, Chen et al. fabricated a tailored carbonate-based electrolyte using  $\text{LiDFBOP}$  for Na metal batteries, where  $\text{DFBOP}^-$  anions can generate stable and robust interphases on both sides and the assembled batteries achieve impressive cycling stability with limited Na.<sup>86</sup> Furthermore, Sahalie et al. and Hagos et al. added  $\text{K}^+$  salts in the conventional electrolytes to introduce a self-healing electrostatic shielding effect to prevent dendrite growth and improve the performance of anode-free configurations.<sup>23,87,88</sup> Tomich et al. designed a fluorine-free electrolyte utilizing the  $[\text{HCB}_{11}\text{H}_{11}]^-$  anion, further demonstrating that Na metal deposition/stripping processes can be mediated by the electrolyte.<sup>89</sup> The corresponding high efficient anode-free configurations benefit from the formation of fluorine-free SEI layer on the surface of Cu/Al foil due to the chemical reduction of diglyme. For solid-state electrolytes, Kim et al. used an in-operando microscopy technique to probe Li deposition through the  $\text{Li}_7\text{La}_3\text{Zr}_2\text{O}_{12}$  (LLZO) electrolyte in an anode-free solid-state battery, where the deposition behavior is mainly affected by the geometry of the LLZO surface.<sup>90</sup> The concentration of Li-ion flux at morphological defective sites of LLZO will accelerate the inhomogeneous deposition, and the modified LLZO surface with an artificial interlayer can regulate Li distribution, further improving the interfacial charge transfer kinetics and the electrochemical performance of the anode-free cell. Li et al. introduced the Pb/C interlayer to resolve the solid-state electrolyte interfacial contact issue by regulating the surface chemistry and improving Na wettability, which exhibits excellent cyclability under the low N/P ratios.<sup>91</sup> The proper dual-salt or multi-salt electrolyte combinations will be beneficial for the improvement of anode-free Na metal batteries, and the design of new salts and solvents with the undiscovered interaction during cycles is worth expecting. The adoption of anode-free Na metal batteries can eliminate sophisticated Na metal lamination and interface modification steps, further reducing the cost and simplifying the processing. However, the same challenges encountered in conventional solid-state electrolytes, such as poor interfacial contacts, space charge effect, and dendritic cell shorting, still apply in anode-free configurations. The ideal interface modification by the construction of an inorganic, organic, or mixed interface buffer layer will be an effective way to optimize solid-state anode-free Na metal batteries.

## SUMMARY AND OPPORTUNITIES

The aim of the anode-free Na metal battery research is to optimize new energy storage systems that compete with Li-ion alternatives in terms of energy density, safety, and cost, but with an even lower environmental impact. As a new technology, testing of anode-free Na metal batteries requires a fundamental reassessment and manufacturing standardization of the new battery chemistry. Especially for some performance parameters, the initial sodium stripping capacity, sodium utilization, theoretical capacity, long-term cycling stability, and fast charging/discharging capability should be clearly clarified. Owing to the lack of excess sodium, how to increase the content of active Na ions in the systems and to improve their utilization is particularly important for anode-free Na metal batteries. The safety and reliability of the final commercialization strategies are paramount to the end-users. Even if they are damaged, abused, or poorly manufactured, they should not ignite or explode. Moreover, the battery design should be optimized for easy disassembly and recycling, which can address many of the current commercial battery recycling challenges.

Although Li-ion batteries are currently the dominant technology in the field of rechargeable batteries, the development of competing chemistries for larger-scale applications is speeding up. The revolution in Na-ion battery strategies is set to change the energy storage market radically, and it will inevitably replace most of the conventional Li-ion battery market. However, the unveiled Na-ion batteries with energy density close to current generation LiFePO<sub>4</sub>-based Li-ion batteries make Na-based strategies less attractive for the wider passenger electric vehicle market. In consideration of the difficulty of Na foil casting as well as the increased safety hazard of the huge excess Na metal in conventional batteries, anode-free Na metal batteries are expected to greatly expand the commercial usage of Na-based batteries due to their low cost, high safety, wide operating temperature range, and more sustainability, which can dominate the rechargeable battery market with energy densities below 250 Wh kg<sup>-1</sup>. To put this into perspective, nearly 54% of transition metal and lithium supply will be released for next-generation high-energy-density Li-ion batteries, further alleviating the shortage of Li, Co, and Ni resources. At the same time, the existing producer surplus would fully house the newly added Na salt and Al supplies for anode-free Na metal batteries. With adequate levels of support, including battery chemistry, cell engineering, and system integration, we conclude that the anode-free Na metal batteries could be operational within the next decade for portable electronics, electric vehicles, and grid energy storage for our society's future.

## ACKNOWLEDGMENTS

This work was supported by the Natural Sciences and Engineering Research Council of Canada (NSERC), Mitacs Accelerate Program, the University of Waterloo, and the Waterloo Institute for Nanotechnology, University of Waterloo.

## AUTHOR CONTRIBUTIONS

T.Y. and D.L. proposed the topic of the work and contributed equally to this work. Y.L. was responsible for image beautification. A.Y. and Z.C. revised the literature and provided the content. Correspondence should be addressed to A.Y. or Z.C. All the authors revised the article and approved the final version of the article.

## DECLARATION OF INTERESTS

The authors declare no competing interests.

## REFERENCES

- Turner, J.M. (2022). The matter of a clean energy future. *Science* 376, 1361. <https://doi.org/10.1126/science.add5094>.
- Viswanathan, V., Epstein, A.H., Chiang, Y.-M., Takeuchi, E., Bradley, M., Langford, J., and Winter, M. (2022). The challenges and opportunities of battery-powered flight. *Nature* 601, 519–525. <https://doi.org/10.1038/s41586-021-04139-1>.
- Gao, H., and Gallant, B.M. (2020). Advances in the chemistry and applications of alkali-metal-gas batteries. *Nat. Rev. Chem* 4, 566–583. <https://doi.org/10.1038/s41570-020-00224-7>.
- Bates, A.M., Preger, Y., Torres-Castro, L., Harrison, K.L., Harris, S.J., and Hewson, J. (2022). Are solid-state batteries safer than lithium-ion batteries? *Joule* 6, 742–755. <https://doi.org/10.1016/j.joule.2022.02.007>.
- IEA (2021). Global EV Outlook 2021 (International Energy Agency). <https://www.iea.org/reports/global-ev-outlook-2021>.
- Sawicki, M., and Shaw, L.L. (2015). Advances and challenges of sodium ion batteries as post lithium ion batteries. *RSC Adv.* 5, 53129–53154. <https://doi.org/10.1039/C5RA08321D>.
- Barnhart, C.J., and Benson, S.M. (2013). On the importance of reducing the energetic and material demands of electrical energy cost of materials for lithium-based rechargeable automotive batteries. *Nat. Energy* 3, 267–278. <https://doi.org/10.1038/s41560-018-0107-2>.

- storage. *Energy Environ. Sci.* 6, 1083–1092. <https://doi.org/10.1039/C3EE24040A>.
- Harper, G., Sommerville, R., Kendrick, E., Driscoll, L., Slater, P., Stolkin, R., Walton, A., Christensen, P., Heidrich, O., Lambert, S., et al. (2019). Recycling lithium-ion batteries from electric vehicles. *Nature* 575, 75–86. <https://doi.org/10.1038/s41586-019-1682-5>.
  - Albertus, P., Babinec, S., Litzelman, S., and Newman, A. (2018). Status and challenges in enabling the lithium metal electrode for high-energy and low-cost rechargeable batteries. *Nat. Energy* 3, 16–21. <https://doi.org/10.1038/s41560-017-0047-2>.
  - Schneider, S.F., Bauer, C., Novák, P., and Berg, E.J. (2019). A modeling framework to assess specific energy, costs and environmental impacts of Li-ion and Na-ion batteries. *Sustain. Energy Fuels* 3, 3061–3070. <https://doi.org/10.1039/C9SE00427K>.
  - Abraham, K.M. (2020). How comparable are sodium-ion batteries to lithium-ion counterparts? *ACS Energy Lett.* 5, 3544–3547. <https://doi.org/10.1021/acsenenergylett.0c02181>.
  - Zhang, W., Lu, J., and Guo, Z. (2021). Challenges and future perspectives on sodium and potassium ion batteries for grid-scale energy storage. *Mater. Today* 50, 400–417. <https://doi.org/10.1016/j.mattod.2021.03.015>.
  - Onstad, E. (2021). CATL's New Sodium Ion Battery To Help Ease Lithium Shortages (Reuters). <https://www.reuters.com/business/energy/catsl-new-sodium-ion-battery-help-ease-lithium-shortages-2021-08-03/>.
  - Frazelle, J. (2020). Battery Day: a closer look at the technology that makes portable electronics possible. *Queue* 18, 5–25. <https://doi.org/10.1145/3434571.3439415>.
  - Nanda, S., Gupta, A., and Manthiram, A. (2021). Anode-free full cells: a pathway to high-energy density lithium-metal batteries. *Adv. Energy Mater.* 11, 2000804. <https://doi.org/10.1002/aenm.202000804>.
  - Nanda, S., Bhargava, A., and Manthiram, A. (2020). Anode-free, lean-electrolyte lithium-sulfur batteries enabled by tellurium-stabilized lithium deposition. *Joule* 4, 1121–1135. <https://doi.org/10.1016/j.joule.2020.03.020>.
  - Qiao, Y., Yang, H., Chang, Z., Deng, H., Li, X., and Zhou, H. (2021). A high-energy-density and long-life initial-anode-free lithium battery enabled by a Li<sub>2</sub>O sacrificial agent. *Nat. Energy* 6, 653–662. <https://doi.org/10.1038/s41560-021-00839-0>.
  - Tian, Y., An, Y., Wei, C., Jiang, H., Xiong, S., Feng, J., and Qian, Y. (2020). Recently advances and perspectives of anode-free rechargeable batteries. *Nano Energy* 78, 105344. <https://doi.org/10.1016/j.nanoen.2020.105344>.
  - Wang, C., Liu, M., Thijs, M., Ooms, F.G.B., Ganapathy, S., and Wagemaker, M. (2021). High dielectric barium titanate porous scaffold for efficient Li metal cycling in anode-free cells. *Nat. Commun.* 12, 6536. <https://doi.org/10.1038/s41467-021-26859-8>.
  - Xie, Z., Wu, Z., An, X., Yue, X., Wang, J., Abudula, A., and Guan, G. (2020). Anode-free rechargeable lithium metal batteries: progress and prospects. *Energy Storage Mater.* 32, 386–401.
  - Zhang, J.-G. (2019). Anode-less. *Nat. Energy* 4, 637–638. <https://doi.org/10.1016/j.ensm.2020.07.004>.
  - Hagos, T.M., Berhe, G.B., Hagos, T.T., Bezabih, H.K., Abrha, L.H., Beyene, T.T., Huang, C.-J., Yang, Y.-W., Su, W.-N., Dai, H., and Hwang, B.J. (2019). Dual electrolyte additives of potassium hexafluorophosphate and tris(trimethylsilyl)phosphite for anode-free lithium metal batteries. *Electrochim. Acta* 316, 52–59. <https://doi.org/10.1016/j.electacta.2019.05.061>.
  - Li, Y., Zhou, Q., Weng, S., Ding, F., Qi, X., Lu, J., Li, Y., Zhang, X., Rong, X., Lu, Y., et al. (2022). Interfacial engineering to achieve an energy density of over 200 Wh kg<sup>-1</sup> in sodium batteries. *Nat. Energy* 7, 511–519. <https://doi.org/10.1038/s41560-022-01033-6>.
  - Usiskin, R., Lu, Y., Popovic, J., Law, M., Balaya, P., Hu, Y.-S., and Maier, J. (2021). Fundamentals, status and promise of sodium-based batteries. *Nat. Rev. Mater.* 6, 1020–1035. <https://doi.org/10.1038/s41578-021-00324-w>.
  - Yang, T., Qian, T., Sun, Y., Zhong, J., Rosei, F., and Yan, C. (2019). Mega high utilization of sodium metal anodes enabled by single zinc atom sites. *Nano Lett.* 19, 7827–7835. <https://doi.org/10.1021/acs.nanolett.9b02833>.
  - Sun, B., Li, P., Zhang, J., Wang, D., Munroe, P., Wang, C., Notten, P.H.L., and Wang, G. (2018). Dendrite-free sodium-metal anodes for high-energy sodium-metal batteries. *Adv. Mater.* 30, 1801334. <https://doi.org/10.1002/adma.201801334>.
  - Wan, M., Kang, S., Wang, L., Lee, H.-W., Zheng, G.W., Cui, Y., and Sun, Y. (2020). Mechanical rolling formation of interpenetrated lithium metal/lithium tin alloy foil for ultrahigh-rate battery anode. *Nat. Commun.* 11, 829. <https://doi.org/10.1038/s41467-020-14550-3>.
  - Wang, A., Hu, X., Tang, H., Zhang, C., Liu, S., Yang, Y.-W., Yang, Q.-H., and Luo, J. (2017). Processable and moldable sodium-metal anodes. *Angew. Chem. Int. Ed. Engl.* 129, 12083–12088. <https://doi.org/10.1002/ange.201703937>.
  - Park, S., Tian, R., Coelho, J., Nicolosi, V., and Coleman, J.N. (2019). Quantifying the trade-off between absolute capacity and rate performance in battery electrodes. *Adv. Energy Mater.* 9, 1901359. <https://doi.org/10.1002/aenm.201901359>.
  - Peters, J., Buchholz, D., Passerini, S., and Weil, M. (2016). Life cycle assessment of sodium-ion batteries. *Energy Environ. Sci.* 9, 1744–1751. <https://doi.org/10.1039/C6EE00640J>.
  - Vaalma, C., Buchholz, D., Weil, M., and Passerini, S. (2018). A cost and resource analysis of sodium-ion batteries. *Nat. Rev. Mater.* 3, 18013. <https://doi.org/10.1038/natrevmats.2018.13>.
  - Morgan, J.W., and Anders, E. (1980). Chemical composition of earth, venus, and mercury. *Proc. Natl. Acad. Sci. USA.* 77, 6973–6977. <https://doi.org/10.1073/pnas.77.12.697>.
  - National Minerals Information Center (2022). Mineral Commodity Summaries 2022. U.S. Geological Survey. <https://doi.org/10.3122/mcs2022>.
  - Fan, E., Li, L., Wang, Z., Lin, J., Huang, Y., Yao, Y., Chen, R., and Wu, F. (2020). Sustainable recycling technology for Li-ion batteries and beyond: challenges and future prospects. *Chem. Rev.* 120, 7020–7063. <https://doi.org/10.1021/acs.chemrev.9b00535>.
  - Chen, M., Ma, X., Chen, B., Arsenaault, R., Karlson, P., Simon, N., and Wang, Y. (2019). Recycling end-of-life electric vehicle lithium-ion batteries. *Joule* 3, 2622–2646. <https://doi.org/10.1016/j.joule.2019.09.014>.
  - Goikolea, E., Palomares, V., Wang, S., Larramendi, I.R., Guo, X., Wang, G., and Rojo, T. (2020). Na-ion batteries—approaching old and new challenges. *Adv. Energy Mater.* 10, 2002055. <https://doi.org/10.1002/aenm.202002055>.
  - IEA (International Energy Agency; 2022). Global Supply Chains of EV Batteries. <https://www.iea.org/reports/global-supply-chains-of-ev-batteries>.
  - Farchy, J., Wong, K., and Burton, M. (2022). Nickel Squeeze Threatens London's Place At Heart Of Metals Trade (Bloomberg News). <https://www.bnnbloomberg.ca/nickel-squeeze-threatens-london-s-place-at-heart-of-metals-trade-1.1739972>.
  - Slater, M.D., Kim, D., Lee, E., and Johnson, C.S. (2013). Sodium-ion batteries. *Adv. Funct. Mater.* 23, 947–958. <https://doi.org/10.1002/adfm.201200691>.
  - Kane, M. (2022). SNE Research: Global xEV Battery Market Exceeded 296 GWh in 2021 (InsideEVs). <https://insideevs.com/news/568640/global-battery-market-2021/>.
  - IEA (2021). Aluminium. International Energy Agency. <https://www.iea.org/reports/aluminium>.
  - Lin, L., Qin, K., Hu, Y.-S., Li, H., Huang, X., Suo, L., and Chen, L. (2022). A better choice to achieve high volumetric energy density: anode-free lithium-metal batteries. *Adv. Mater.* 34, e2110323. <https://doi.org/10.1002/adma.202110323>.
  - Zhao, S., Yan, K., Zhang, J., Sun, B., and Wang, G. (2021). Reaction mechanisms of layered lithium-rich cathode materials for high-energy lithium-ion batteries. *Angew. Chem. Int. Ed. Engl.* 60, 2208–2220. <https://doi.org/10.1002/anie.202000262>.
  - Zuo, W., Luo, M., Liu, X., Wu, J., Liu, H., Li, J., Winter, M., Fu, R., Yang, W., and Yang, Y.

- (2020). Li-rich cathodes for rechargeable Li-based batteries: reaction mechanisms and advanced characterization techniques. *Energy Environ. Sci.* 13, 4450–4497. <https://doi.org/10.1039/D0EE01694B>.
46. Li, C., Geng, F., Hu, B., and Hu, B. (2020). Anionic redox in Na-based layered oxide cathodes: a review with focus on mechanism studies. *Mater. Today Energy* 17, 100474. <https://doi.org/10.1016/j.mtener.2020.100474>.
47. Park, J., Ko, I., Lee, J., Park, S., Kim, D., Yu, S., and Sung, Y. (2021). Anionic redox reactions in cathodes for sodium-ion batteries. *ChemElectroChem* 8, 625–643. <https://doi.org/10.1002/celec.202001383>.
48. Yu, Y., Ning, D., Li, Q., Franz, A., Zheng, L., Zhang, N., Ren, G., Schumacher, G., and Liu, X. (2021). Revealing the anionic redox chemistry in O<sub>3</sub>-type layered oxide cathode for sodium-ion batteries. *Energy Storage Mater.* 38, 130–140. <https://doi.org/10.1016/j.ensm.2021.03.004>.
49. Xu, H., Guo, S., and Zhou, H. (2019). Review on anionic redox in sodium-ion batteries. *J. Mater. Chem.* 7, 23662–23678. <https://doi.org/10.1039/C9TA06389G>.
50. Tang, X., Liu, H., Su, D., Notten, P.H.L., and Wang, G. (2018). Hierarchical sodium-rich Prussian blue hollow nanospheres as high-performance cathode for sodium-ion batteries. *Nano Res.* 11, 3979–3990. <https://doi.org/10.1007/s12274-018-1979-y>.
51. Wang, W., Gang, Y., Hu, Z., Yan, Z., Li, W., Li, Y., Gu, Q.-F., Wang, Z., Chou, S.-L., Liu, H.-K., and Dou, S.X. (2020). Reversible structural evolution of sodium-rich rhombohedral Prussian blue for sodium-ion batteries. *Nat. Commun.* 11, 980. <https://doi.org/10.1038/s41467-020-14444-4>.
52. Park, M.-S., Lim, Y.-G., Kim, J.-H., Kim, Y.-J., Cho, J., and Kim, J.-S. (2011). A novel lithium-doping approach for an advanced lithium-ion capacitor. *Adv. Energy Mater.* 1, 1002–1006. <https://doi.org/10.1002/aenm.201100270>.
53. Zhang, S.S., Fan, X., and Wang, C. (2018). An in-situ enabled lithium metal battery by plating lithium on a copper current collector. *Electrochem. Commun.* 89, 23–26. <https://doi.org/10.1016/j.elecom.2018.02.011>.
54. Park, K.-S., Im, D., Benayad, A., Dylla, A., Stevenson, K.J., and Goodenough, J.B. (2012). LiFeO<sub>2</sub>-incorporated Li<sub>2</sub>MoO<sub>3</sub> as a cathode additive for lithium-ion battery safety. *Chem. Mater.* 24, 2673–2683. <https://doi.org/10.1021/cm300505y>.
55. Ye, M., You, S., Xiong, J., Yang, Y., Zhang, Y., and Li, C.C. (2022). In-situ construction of a NaF-rich cathode-electrolyte interface on Prussian blue toward a 3000-cycle-life sodium-ion battery. *Mater. Today Energy* 23, 100898. <https://doi.org/10.1016/j.mtener.2021.100898>.
56. Hu, P., Peng, W., Wang, B., Xiao, D., Ahuja, U., Réthoré, J., and Afifants, K.E. (2020). Concentration-gradient prussian blue cathodes for Na-ion batteries. *ACS Energy Lett.* 5, 100–108. <https://doi.org/10.1021/acscenergylett.9b02410>.
57. Gebert, F., Cortie, D.L., Bouwer, J.C., Wang, W., Yan, Z., Dou, S.-X., and Chou, S.-L. (2021). Epitaxial nickel ferrocyanide stabilizes jahn-teller distortions of manganese ferrocyanide for sodium-ion batteries. *Angew. Chem. Int. Ed. Engl.* 60, 18519–18526. <https://doi.org/10.1002/ange.202106240>.
58. Li, M., Wang, C., Chen, Z., Xu, K., and Lu, J. (2020). New concepts in electrolytes. *Chem. Rev.* 120, 6783–6819. <https://doi.org/10.1021/acs.chemrev.9b00531>.
59. Borodin, O., Self, J., Persson, K.A., Wang, C., and Xu, K. (2020). Uncharted waters: superconcentrated electrolytes. *Joule* 4, 69–100. <https://doi.org/10.1016/j.joule.2019.12.007>.
60. Dubouis, N., Marchandier, T., Rousse, G., Marchini, F., Fauth, F., Avdeev, M., Iadecola, A., Porcheron, B., Deschamps, M., Tarascon, J.-M., and Grimaud, A. (2021). Extending insertion electrochemistry to soluble layered halides with superconcentrated electrolytes. *Nat. Mater.* 20, 1545–1550. <https://doi.org/10.1038/s41563-021-01060-w>.
61. Hwang, J., Sivasengaran, A.N., Yang, H., Yamamoto, H., Takeuchi, T., Matsumoto, K., and Hagiwara, R. (2021). Improvement of electrochemical stability using the eutectic composition of a ternary molten salt system for highly concentrated electrolytes for Na-ion batteries. *ACS Appl. Mater. Interfaces* 13, 2538–2546. <https://doi.org/10.1021/acscami.0c17807>.
62. Qian, J., Adams, B.D., Zheng, J., Xu, W., Henderson, W.A., Wang, J., Bowden, M.E., Xu, S., Hu, J., and Zhang, J.-G. (2016). Anode-free rechargeable lithium metal batteries. *Adv. Funct. Mater.* 26, 7094–7102. <https://doi.org/10.1002/adfm.201602353>.
63. Beyene, T.T., Jote, B.A., Wondimkun, Z.T., Olbassa, B.W., Huang, C.-J., Thirumalraj, B., Wang, C.-H., Su, W.-N., Dai, H., and Hwang, B.-J. (2019). Effects of concentrated salt and resting protocol on solid electrolyte interface formation for improved cycle stability of anode-free lithium metal batteries. *ACS Appl. Mater. Interfaces* 11, 31962–31971. <https://doi.org/10.1021/acscami.9b09551>.
64. Huang, C.-J., Thirumalraj, B., Tao, H.-C., Shitaw, K.N., Sutiono, H., Hagos, T.T., Beyene, T.T., Kuo, L.-M., Wang, C.-C., Wu, S.-H., et al. (2021). Decoupling the origins of irreversible coulombic efficiency in anode-free lithium metal batteries. *Nat. Commun.* 12, 1452. <https://doi.org/10.1038/s41467-021-21683-6>.
65. Sun, J., O'Dell, L.A., Armand, M., Howlett, P.C., and Forsyth, M. (2021). Anion-derived solid-electrolyte interphase enables long life Na-ion batteries using superconcentrated ionic liquid electrolytes. *ACS Energy Lett.* 6, 2481–2490. <https://doi.org/10.1021/acscenergylett.1c00816>.
66. Lu, Z., Yang, H., Yang, Q.-H., He, P., and Zhou, H. (2022). Building a beyond concentrated electrolyte for high-voltage anode-free rechargeable sodium batteries. *Angew. Chem. Int. Ed. Engl.* 61, e202200410. <https://doi.org/10.1002/ange.202200410>.
67. Chen, F., Howlett, P., and Forsyth, M. (2018). Na-ion solvation and high transference number in superconcentrated ionic liquid electrolytes: a theoretical approach. *J. Phys. Chem. C* 122, 105–114. <https://doi.org/10.1021/acs.jpcc.7b09322>.
68. Zhao, Y., Adair, K.R., and Sun, X. (2018). Recent developments and insights into the understanding of Na metal anodes for Na-metal batteries. *Energy Environ. Sci.* 11, 2673–2695. <https://doi.org/10.1039/C8EE01373J>.
69. Xia, X., Du, C., Zhong, S., Jiang, Y., Yu, H., Sun, W., Pan, H., Rui, X., and Yu, Y. (2022). Homogeneous Na deposition enabling high-energy Na-metal batteries. *Adv. Funct. Mater.* 32, 2110280. <https://doi.org/10.1002/adfm.202110280>.
70. Liu, T., Yang, X., Nai, J., Wang, Y., Liu, Y., Liu, C., and Tao, X. (2021). Recent development of Na metal anodes: interphase engineering chemistries determine the electrochemical performance. *Chem. Eng. J.* 409, 127943. <https://doi.org/10.1016/j.cej.2020.127943>.
71. Luo, W., Lin, C., Zhao, O., Noked, M., Zhang, Y., Rubloff, G.W., and Hu, L. (2017). Ultrathin surface coating enables the stable sodium metal anode. *Adv. Energy Mater.* 7, 1601526. <https://doi.org/10.1002/aenm.201601526>.
72. Tian, H., Seh, Z.W., Yan, K., Fu, Z., Tang, P., Lu, Y., Zhang, R., Legut, D., Cui, Y., and Zhang, Q. (2017). Theoretical investigation of 2D layered materials as protective films for lithium and sodium metal anodes. *Adv. Energy Mater.* 7, 1602528. <https://doi.org/10.1002/aenm.201602528>.
73. Snyder, D.H., Hegde, V.I., and Wolverton, C. (2017). Electrochemically stable coating materials for Li, Na, and Mg metal anodes in durable high energy batteries. *J. Electrochem. Soc.* 164, A3582–A3589. <https://doi.org/10.1149/2.0371714jes>.
74. Wang, Y., Dong, H., Katyal, N., Hao, H., Liu, P., Celio, H., Henkelman, G., Watt, J., and Mitlin, D. (2022). A sodium-antimony-telluride intermetallic allows sodium-metal cycling at 100% depth of discharge and as an anode-free metal battery. *Adv. Mater.* 34, 2106005. <https://doi.org/10.1002/adma.202106005>.
75. Hou, Z., Wang, W., Yu, Y., Zhao, X., Chen, Q., Zhao, L., Di, Q., Ju, H., and Quan, Z. (2020). Poly(vinylidene difluoride) coating on Cu current collector for high-performance Na metal anode. *Energy Storage Mater.* 24, 588–593. <https://doi.org/10.1016/j.ensm.2019.06.026>.
76. Jung, J., Hwang, D.Y., Kristanto, I., Kwak, S.K., and Kang, S.J. (2019). Deterministic growth of a sodium metal anode on a pre-patterned current collector for highly rechargeable seawater batteries. *J. Mater. Chem.* 7, 9773–9781. <https://doi.org/10.1039/C9TA01718F>.
77. Cohn, A.P., Muralidharan, N., Carter, R., Share, K., and Pint, C.L. (2017). Anode-free sodium battery through in situ plating of sodium metal. *Nano Lett.* 17, 1296–1301.

- <https://doi.org/10.1021/acs.nanolett.6b05174>.
78. Mazzali, F., Orzech, M.W., Adomkevicius, A., Pisanu, A., Malavasi, L., Deganello, D., and Margadonna, S. (2019). Designing a high-power sodium-ion battery by in situ metal plating. *ACS Appl. Energy Mater.* **2**, 344–353. <https://doi.org/10.1021/acsaem.8b01361>.
79. Tang, S., Qiu, Z., Wang, X.-Y., Gu, Y., Zhang, X.-G., Wang, W.-W., Yan, J.-W., Zheng, M.-S., Dong, Q.-F., and Mao, B.-W. (2018). A room-temperature sodium metal anode enabled by a sodiophilic layer. *Nano Energy* **48**, 101–106. <https://doi.org/10.1016/j.nanoen.2018.03.039>.
80. Lee, M.E., Kwak, H.W., Kwak, J.H., Jin, H.-J., and Yun, Y.S. (2019). Catalytic pyroprotein seed layers for sodium metal anodes. *ACS Appl. Mater. Interfaces* **11**, 12401–12407. <https://doi.org/10.1021/acsami.8b15938>.
81. Zhao, Y., Goncharova, L.V., Lushington, A., Sun, Q., Yadegari, H., Wang, B., Xiao, W., Li, R., and Sun, X. (2017). Superior stable and long life sodium metal anodes achieved by atomic layer deposition. *Adv. Mater.* **29**, 1606663. <https://doi.org/10.1002/adma.201606663>.
82. Li, H., Zhang, H., Wu, F., Zarrabeitia, M., Geiger, D., Kaiser, U., Varzi, A., and Passerini, S. (2022). Sodiophilic current collectors based on MOF-derived nanocomposites for anode-less Na-metal batteries. *Adv. Energy Mater.* **12**, 2202293. <https://doi.org/10.1002/aenm.202202293>.
83. Louli, A.J., Eldesoky, A., Weber, R., Genovese, M., Coon, M., deGooyer, J., Deng, Z., White, R.T., Lee, J., Rodgers, T., et al. (2020). Diagnosing and correcting anode-free cell failure via electrolyte and morphological analysis. *Nat. Energy* **5**, 693–702. <https://doi.org/10.1038/s41560-020-0668-8>.
84. Eldesoky, A., Louli, A.J., Benson, A., and Dahn, J.R. (2021). Cycling performance of NMC811 anode-free pouch cells with 65 different electrolyte formulations. *J. Electrochem. Soc.* **168**, 120508. <https://doi.org/10.1149/1945-7111/ac39e3>.
85. Weber, R., Genovese, M., Louli, A.J., Hames, S., Martin, C., Hill, I.G., and Dahn, J.R. (2019). Long cycle life and dendrite-free lithium morphology in anode-free lithium pouch cells enabled by a dual-salt liquid electrolyte. *Nat. Energy* **4**, 683–689. <https://doi.org/10.1038/s41560-019-0428-9>.
86. Chen, J., Peng, Y., Yin, Y., Liu, M., Fang, Z., Xie, Y., Chen, B., Cao, Y., Xing, L., Huang, J., et al. (2022). High energy density Na-metal batteries enabled by a tailored carbonate-based electrolyte. *Energy Environ. Sci.* **15**, 3360–3368. <https://doi.org/10.1039/D2EE01257J>.
87. Sahalie, N.A., Assegie, A.A., Su, W.-N., Wondimkun, Z.T., Jote, B.A., Thirumalraj, B., Huang, C.-J., Yang, Y.-W., and Hwang, B.-J. (2019). Effect of bifunctional additive potassium nitrate on performance of anode free lithium metal battery in carbonate electrolyte. *J. Power Sources* **437**, 226912. <https://doi.org/10.1016/j.jpowsour.2019.226912>.
88. Tan, D.H.S., Banerjee, A., Chen, Z., and Meng, Y.S. (2020). From nanoscale interface characterization to sustainable energy storage using all-solid-state batteries. *Nat. Nanotechnol.* **15**, 170–180. <https://doi.org/10.1038/s41565-020-0657-x>.
89. Tomich, A.W., Park, J., Son, S.-B., Kamphaus, E.P., Lyu, X., Dogan, F., Carta, V., Gim, J., Li, T., Cheng, L., et al. (2022). A carboranyl electrolyte enabling highly reversible sodium metal anodes via a “Fluorine-Free” SEI. *Angew. Chem. Int. Ed. Engl.* **61**, e202208158. <https://doi.org/10.1002/anie.202208158>.
90. Kim, S., Jung, C., Kim, H., Thomas-Alyea, K.E., Yoon, G., Kim, B., Badding, M.E., Song, Z., Chang, J., Kim, J., et al. (2020). The role of interlayer chemistry in Li-metal growth through a garnet-type solid electrolyte. *Adv. Energy Mater.* **10**, 1903993. <https://doi.org/10.1002/aenm.201903993>.
91. Li, R., Jiang, D., Du, P., Yuan, C., Cui, X., Tang, Q., Zheng, J., Li, Y., Lu, K., Ren, X., et al. (2022). Negating Na||Na<sub>3</sub>Zr<sub>2</sub>Si<sub>2</sub>PO<sub>12</sub> interfacial resistance for dendrite-free and “Na-less” solid-state batteries. *Chem. Sci.* **13**, 14132–14140. <https://doi.org/10.1039/D2SC05120F>.